Experimental and Numerical Simulation of Brinell Hardness Test of Al7075 Alclad T6 in Abaqus

A. Wakeel[1], M. A. Nasir[2], R. A. Pasha[3], N. A. Anjum[4], J. Shafique[5]

Department of Mechanical Engineering, University of Engineering & Technology, Taxila, Pakistan
[2]ali.nasir@uettaxila.edu.pk

Abstract-Aerospace technology widely depend on the Strength-to-Density ratio of materials and Aluminum Alloys (Usually Al-7075 T6) is generally playing vital role in fulfilling these requirements. Al-7075 is often used in transport applications, including marine, automotive and aviation. Computer simulation is a popular instrument in the field of engineering to visualize the material behaviour. The phenomenon of indentation deformation is examined utilizing FEA for homogeneous materials. Thus this work describe the experimental and numerical simulation of indentation of (spherical) steel ball indenter on Al 7075 T6 Alclad and measure the hardness of that Al alloy by experimentally and numerically. The main objective is to compare the hardness of that material by experimentation and numerical simulation in Abaqus. This study shows that the numerical simulation result in ABAQUS are more accurate than experimental results.

Keywords-Numerical Simulation, Indentation, Spherical Indenter, Hardness

I. INTRODUCTION

Hardness is the property of a material that empowers it to oppose plastic deformation, entrance, indentation, and scratching. Hardness tests serve a vital need in industry despite the fact that they don't quantify an extraordinary quality that can be named hardness. FEM has been connected to indentation estimations to help comprehend the indentation procedure and enhance the precision of the investigative techniques.

The researcher utilized the FEM to think about the indentation analyze [i-ii]. A simulation on tapered indentation was performed boundary component finite element simulation of Berkovich indentation [iii]. The indentation load depth bends were acquired and after that contrasted with exploratory estimations. A comparable report was directed later by reference [iv] utilizing FEM and the impact of indenter tip roundness on indentation estimation was exhaustively examined.

Numerical investigation has turned into a noteworthy procedure to think about the indentation deformation of elasto-plastic materials [v-xii]. They directed the finite element simulation on spherical indentation [xiii]. Also another researcher utilized the FEM to consider the friction and sliding/staying wonders amongst indenter and example [xiv]. The formation of crack created in these materials was likewise talked about.

The vast majority of the investigations said above have been focused around relative shallower indentation. There is little investigation on deeper indentation of elastic plastic materials analyses have been carried out.

II. EXPERIMENTAL SECTION

A. Brinell Hardness Test

For Brinell hardness test, the hardness of materials are test by squeezing a steel ball or tungsten carbide ball for a period of 10 to 14 seconds into the surface of test metal by a standard load F [kgf]. From that point onward, the diameter d [mm] is measured when the load is expelled. The Brinell hardness number HB, is gotten by separating the span of the load connected by the surface area of the circular space A [mm^2]. Where d (mm) is the depth of indentation, D (mm) is the measurement of the ball. For delicate or hard materials, the Brinell test can't be utilized. This test is restricted to materials with hardness up to 450 HB with a steel ball indenter and 600 HB with a tungsten carbide ball indenter.

Fig. 1. Hardness Testing Machine

The standard ISO 6506-1 was taken after to play out that test. For Aluminum alloys the indenter will be utilized of steel ball having distance across 5.0mm and force of 613 N is connected for indentation. In the wake of performing Brinell hardness test, measure the mean distance across of Indentation that is 0.74mm and after that ascertain BHN by utilizing following formula:

$$BHN = \frac{2P}{\pi D \left(D - \sqrt{D^2 - d^2} \right)} \quad (1)$$

The Aluminum 7075 T6 Alclad plate which is used for Brinell hardness test is as follow:

Fig. 2. Tested samples of Al 7075 T6 Alclad

TABLE I
BHN VALUE OF DIFFERENT SAMPLES

Sample	BHN1	BHN2	BHN3	Avg. BHN
1H	144	146.1	143.4	144.6
2H	140.2	148	144	144.1
3H	143	145	144.9	144.3

The mean hardness number which is calculated by brinell hardness test experimentally is 144.3.

III. NUMERICAL SIMULATION

A. Indenter and specimen contact model

Fig. 3. Indenter and a specimen contact model in Abaqus

To examine the elastic plastic distortion of strong homogeneous materials. In this model an indenter is pushed against a deformable test metal by applying a load on the focal point of the sphere. The circle (ball) entered into a level like in a space procedure. It is expected that the material of the indenter is harder than the material of the test metal. The indenter size of sweep is 0.5 mm (1/16 inch like in Brinell hardness test) and the level size is 100 mm length and 6 mm thickness.

B. Material Properties

The material properties are choosen based on the elastic modulus and the values of yield strength. Table shows the materials used for the simulation of contact problems and the Brinell hardness test.

Elastic modulus= 71GPa
Poisson ratio=0.33

The values of yield stress across the plastic strain from tensile testing from that graph
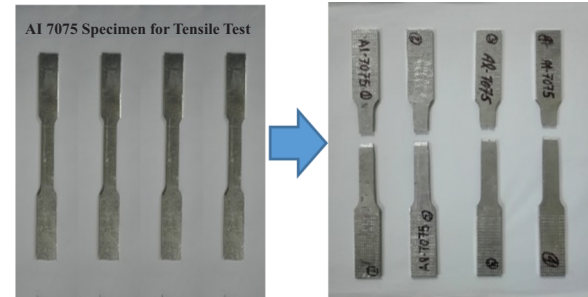
Fig. 4. Before and after tensile testing specimen

The graph obtaining between true stress and true strain after tensile testing is
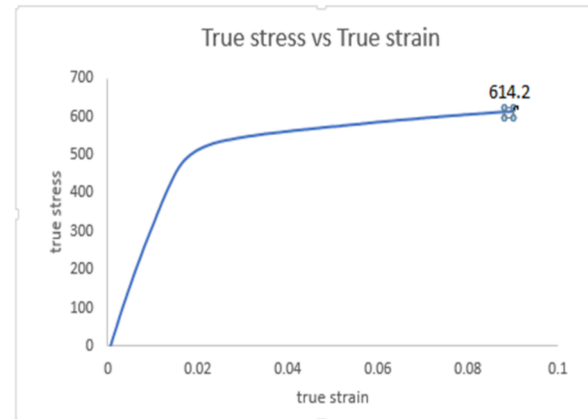
Fig. 5. plot between true stress vs true strain

C. Boundary Condition and Loading

Fig. 6. Boundary conditions and loading

Fig. 6 demonstrates the boundary condition and loading for the simulation of given problem. The nodes lying on the axis of symmetry of the level removal are confined to move in the radially (U1= UR3 = 0). Additionally the nodes in the base of the level removal are limited to move in the vertically (U2 = 0). In the rigid surface the interpretations and pivots on a single node is known as inflexible body reference node. The boundary conditions connected for this point are confined to move outspread way (U1 = UR3 = 0).

D.   Mesh Generation
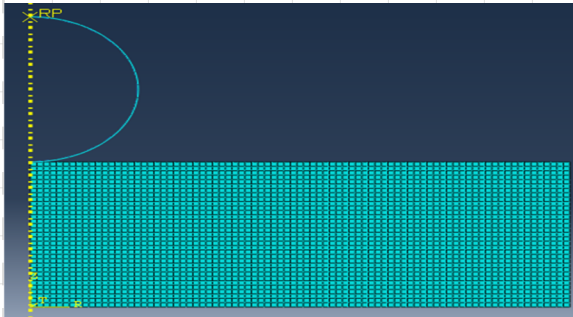
Fig. 7. Mesh generation

The edges of the specimen are mesh by one-sided seed edges technique. The better mesh is created around the indenter with a specific end goal to incorporate the district of the higher worry close to the contact as appeared in Fig. 7. The component type of CAX4R sort was utilized for every one of the simulation in which the letter or number shows the kind of component which is of Continuum type.

E.   Loading Condition

The finite element simulations has been performed by utilizing the state of frictionless contact between the indenter and the level for circular indentation approach. The indentation procedure is thought to be semi static approach, in which no time impact is considered. Consequently ABAQUS - Standard strategy is utilized for indentation approach. The versatile plastic material models is examined

IV. RESULTS AND DISCUSSION

A.   Simulation output for Aluminum 7075 T6 Alclad

The following are the simulation results of Aluminum 7075 T6 Alclad material for an indentation depth of 1mm in ABAQUS Standard
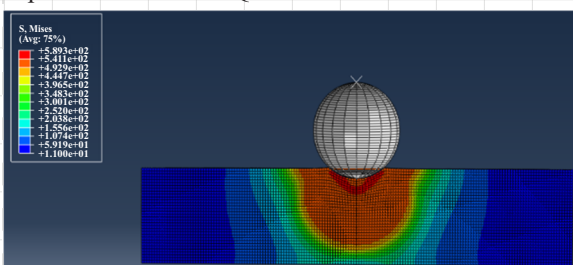
Fig. 8. Misses Stress in the deformed Aluminum 7075 T6 Alclad

Fig. 8 demonstrates the Misses stress created in the deformed flat. The maximum stress is created in the contact area between indenter and the flat. The minimum stress is far away from the contact region. The values of maximum and minimum stresses are 589.3 N/mm^2 and 0.1120 N/mm^2.
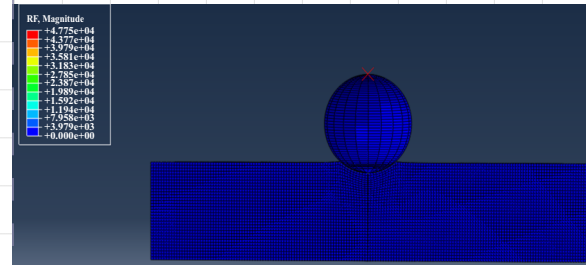
Fig. 9. Reaction force in the indentation into a Aluminum 7075 T6 Alclad.

Fig. 9 demonstrates the reaction force   created in the rigid spherical indenter. In the displacement control procedure, for RF on the indenter is the summation of force over the contact zone along the penetration direction. The reaction force in the indenter is 4775.6 N.
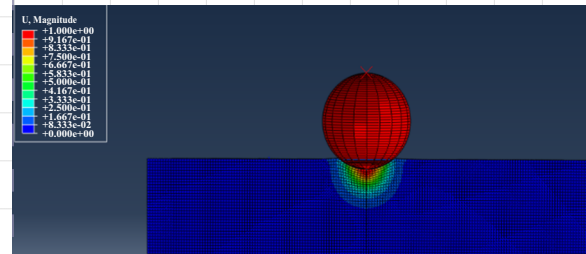
Fig. 10. Displacement of nodes in the Y-direction of Aluminum 7075 T6 Alclad

Fig. 10 demonstrates that displacement of nodes in the loaded flat. Maximum was at the edge of the contact and the minimum displacement of the nodes was under the indenter. The displacement of nodes which was under the tip of the indenter is nearly equal to the displacement of the indenter.
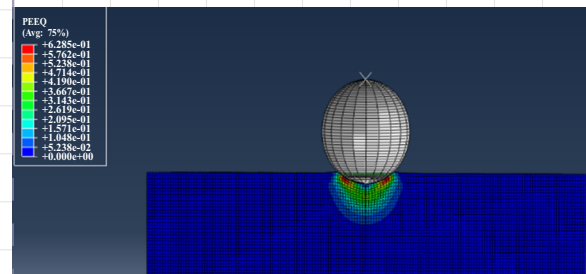
Fig. 11. Equivalent plastic strain plot of Aluminum 7075 T6 Alclad

Figure demonstrates the scalar plastic strain that was created in the model. PEEQ is actually an

integrated estimation of plastic strain. The graph demonstrates the deformed shape of the loaded flat. The maximum plastic strain is created in the flat and it was under the indenter. The zero plastic strain was in outside region the contact zone.
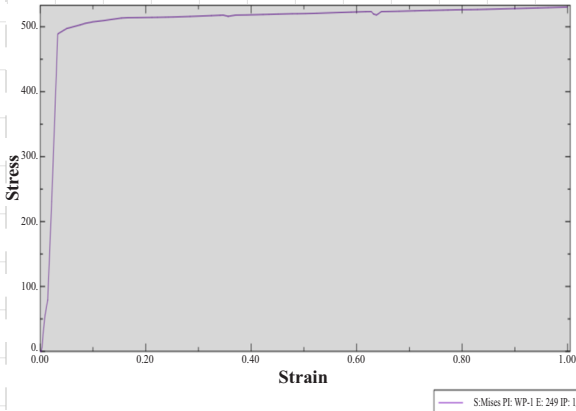
Fig. 12. True stress vs True plastic strain for Aluminum 7075 T6 Alclad

Fig. 12 demonstrates the True stress and True plastic strain for the material Young's modulus estimation of 71×10^9 N/mm2 and initial yield strength estimation of 510.2MPa. The True stress and True plastic strain are figured from the nominal stress and strain respectively.
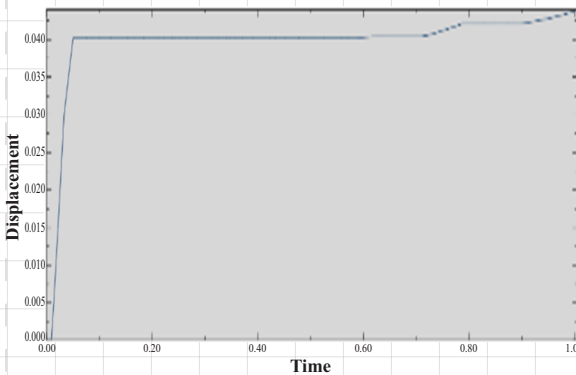
Fig. 13. Graph for displacement of rigid indenter with time into an Al 7075 T6 Alclad.

Fig. 13 demonstrates the simulation yield plot of displacement of spherical indenter reference point. This plot gives the connection between the displacement of indenter vertical way to infiltrated into a steel flat and % of indenter movement into the flat. This plot is a proof for the spherical indenter is totally (100%) infiltrated into a steel flat for the given indenter uprooting of 0.13 mm. It is obviously demonstrated that, the indenter is step by step (direct) infiltrated into a level when the % of the indenter movement is come to up to 100%.

V. IMAGE ANALYSIS FOR NUMERICAL VALUE OF BRINELL HARDNESS
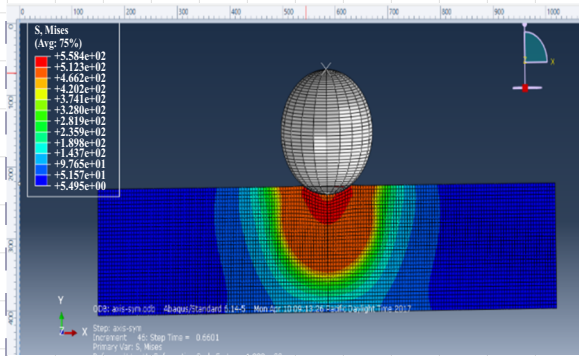
Fig. 14. Image analysis in paint

To calculate the original length of the circle we use the distance formula, i.e

$$Distance = \sqrt{(x_1 - x_2)^2 + (y_1 - y_2)^2} \quad (2)$$

From the Fig.;
X_1=540 px Y_1= 228 px
X_2= 630 px Y_2= 228 px
Distance = $\sqrt{(540-630)^2 + (228-228)^2}$
$\qquad$ =90 px
Scale Conversion
$\quad$ No. of pixels per mm = 1070-450
$\qquad\qquad\qquad\qquad$ = 620
$\qquad\qquad\qquad\qquad$ =620/5
$\qquad$ (5 mm is the thickness of the specimen)
$\qquad\qquad\qquad\qquad$ =124 px/mm
$\qquad\qquad$ Total pixels = 90 px
$\qquad\qquad$ Original Length = 90/124
$\qquad\qquad$ =0.725 mm
This is basically diameter of indentation in numerical simulation. By putting the values of diameter of indentation and other known parameter which is force and diameter of indenter, calculate the Brinell hardness number using Eq. 1. The Small d is 0.725 mm evaluated from image analysis.

The hardness number which is calculated by brinell hardness test numerically simulated is 150.61.

VI. CONCLUSION

The simulation has been performed in the "ABAQUS" for the spherical indentation demonstrate. The ABAQUS software is utilized for simulation having the benefit of restarting the information for unloading process. The investigation was done for the aluminum 7075 T6 Alclad at various indentation depth under loading and unloading conditions. The response force in the unbending indenter and indentation diameter are evaluated in the loading condition. The FEA has been utilized to simulate the deep indentation

of strain-hardening, elastoplastic materials by an unbending, spherical indenter. As an analytical tool, simulation helps to lower the cost and duration of experimental studies by safe and fast computations.

As usual as we concluded that the numerical simulation gives more accurate results than the experimental results in short time. This implies that the suggested simulation tool is adequate for solving problems of hardness profiles of a material.

REFERENCE

[i]   A. K. Bhattacharya and W. D. Nix, *Finite element simulation of indentation experiments.* International Journal of Solids and Structures, 1988. 24(9): p. 881-891.

[ii]   A. K. Bhattacharya and W. D. Nix, *Finite element analysis of cone indentation.* International Journal of Solids and Structures, 1991. 27(8): p. 1047-1058.

[iii]   P.-L.Larsson, A. E. Giannakopoulos, E. SÖderlund, D. J. RowcliffeR. Vestergaard., *Analysis of Berkovich indentation.* International Journal of Solids and Structures, 1996. 33(2): p. 221-248.

[iv]   Y. T. Cheng and C. M. Cheng, *Further analysis of indentation loading curves: Effects of tip rounding on mechanical property measurements.* Journal of Materials research, 1998. 13(4): p. 1059-1064.

[v]   X. Cai, *Effect of friction in indentation hardness testing: a finite element study.* Journal of materials science letters, 1993. 12(5): p. 301-302.

[vi]   K. Sadeghipour, W. Chen, and G. Baran, *Spherical micro-indentation process of polymer-based materials: a finite element study.* Journal of Physics D: Applied Physics, 1994. 27(6): p. 1300.

[vii]   C. Shih, M. Yang, and J. C. M. Li, *Effect of tip radius on nanoindentation.* Journal of materials research, 1991. 6(12): p. 2623-2628.

[viii] J. Shu and N. A. Fleck, *The prediction of a size effect in microindentation.* International Journal of Solids and Structures, 1998. 35(13): p. 1363-1383.

[ix]   B. Taljat, T. Zacharia, and F. Kosel, *New analytical procedure to determine stress-strain curve from spherical indentation data.* International Journal of Solids and Structures, 1998. 35(33): p. 4411-4426.

[x]   F. Yang, J. C. M. Li, and C. W. Shih, *Computer simulation of impression creep using the hyperbolic sine stress law.* Materials Science and Engineering: A, 1995. 201(1-2): p. 50-57.

[xi]   F. Yang, *Indentation of an incompressible elastic film.* Mechanics of Materials, 1998. 30(4): p. 275-286.

[xii]   F. Yang, and A. Saran, *Cyclic indentation of an elastic-perfectly plastic material.* Journal of materials science, 2006. 41(18): p. 6077-6080.

[xiii] S. D. Mesarovic, and N. A. Fleck. *Spherical indentation of elastic–plastic solids.* in *Proceedings of the Royal Society of London A: Mathematical, Physical and Engineering Sciences.* 1999. The Royal Society.

[xiv]   S. Hainsworth, T. Bartlett, and T. Page, *The nanoindentation response of systems with thin hard carbon coatings.* Thin Solid Films, 1993. 236(1-2): p. 214-218.